Cross-validation of the DEM obtained using LuTan-1 SAR satellites: A case study in Guyuan County, China

Xinming Tang [1], Yao Lu [1, *], Tao Li [1], Xiaoqing Zhou [1], Jing Lu [1], Xiang Zhang [1], Xuefei Zhang [1], Xiaofeng Qiu [2], Jiyi Chen [1]
[1] Land Satellite Remote Sensing Application Center, Ministry of Natural Resources, Beijing, China - luyao8899@qq.com
[2] Beijing SatImage Information Technology Co.,Ltd., Beijing 100048, China - 1040706520@qq.com

Keywords: LuTan-1, GaoFen-7, Digital Elevation Model, Cross-validation.

Abstract

The digital elevation model (DEM) based on synthetic aperture radar interferometry (SAR, InSAR) technology have become an important data source for large-scale topographic mapping, but their characteristics vary with satellite systems and methodologies. In this paper, we conduct the cross-validation for the first time to compare the LuTan-1 raw DEM (LT-1 RDEM) and GaoFen-7 (GF-7) satellite laser altimetry data. Besides, we compared the penetration capabilities of SAR satellites including C-band SRTM and X-band TanDEM-X. The optically derived ZiYuan-3 (ZY-3) DEM was also included for multi-source cross-validation. Taking Guyuan County, Hebei Province, China (including four landform types: plains, tablelands, hills, and mountains) as the study area, we introduced GF-7 laser altimetry points (LAPs) as the verification benchmark to cross-validate the elevation accuracy of LT-1 RDEM, SRTM, TanDEM-X DEM (TanDEM), and ZY-3 DEM. The results indicate that: (1) Topographic relief has a significant impact on accuracy, and the RMSE of the DEMs in the study area generally increases sequentially with the intensification of topographic relief; (2) Benefiting from the 10-meter spatial resolution, LT-1 RDEM performs best in detail representation; (3) In terms of mean height error, LT-1 RDEM exhibits a general negative bias, confirming the stronger penetration capability of the L-band, and its elevation values may be closer to the true ground surface; (4) The RMSE of LT-1 RDEM in the study area is 1.958m, slightly larger than TanDEM’s 1.65m, but in fact, the accuracy of TanDEM as a digital surface model (DSM) may be systematically overestimated by laser altimetry data.

1. Introduction

The digital elevation model (DEM) serves as a fundamental representation of terrain elevation and constitutes core data within geospatial databases. It is widely applied in various fields such as terrain analysis, earthwork calculation, flood storage capacity estimation, and geohazard assessment (Tang et al., 2021). Large-scale DEMs are primarily generated through several techniques, including interferometric synthetic aperture radar (SAR, InSAR) (Eldhuset et al., 2003), optical stereo-pair imaging (Takaku et al., 2016), and light detection and ranging (LiDAR) (Liu et al., 2005). Among these, InSAR has rapidly emerged as a key research focus for large-scale DEM acquisition due to its all-weather capability, active imaging, and penetration through clouds (Hong & Yang, 2018; Wecklich et al., 2017). In terms of data sources, scholars have predominantly utilized satellite data such as Sentinel-1A (Karabörk et al., 2021), Gaofen-3 (H. Lu et al., 2018), ALOS PALSAR (Wei et al., 2013), and TerraSAR-X/TanDEM-X (Leonardo et al., 2020). Currently, the satellite missions capable of global DEM production include C-band SRTM, X-band TanDEM-X, and L-band LuTan-1 (LT-1).

Regarding accuracy validation and analysis, most studies employ global navigation satellite system (GNSS) coordinates obtained from field surveys (Apeh et al., 2019; Zhao et al., 2011) or airborne LiDAR data as reference datasets (Shangmin et al., 2020; Uuemaa et al., 2020). Some studies have also adopted satellite laser altimetry data, such as Ice, Cloud, and land Elevation Satellite-2 (ICESat-2) (H. Li et al., 2022; Shuangcheng et al., 2025). However, to date, no research has utilized Gaofen-7 (GF-7) laser altimetry data for validating the accuracy of LT-1-derived DEM.

LT-1 is China's first L-band differential interferometric SAR satellite constellation with interferometric applications as its core mission, consisting of two satellites (LT-1A and LT-1B) (T. Li et al., 2023). LT-1A and LT-1B were successfully launched from the Jiuquan Satellite Launch Center in China on January 26 and February 27, 2022, respectively. Operating in a quasi-sun-synchronous orbit at an altitude of 607 kilometers, they are equipped with advanced L-band multi-polarization and multi-channel SAR payloads, featuring multiple imaging modes, a maximum resolution of 3 meters, and a maximum swath width of up to 400 kilometers. The two satellites operate in a formation configuration, offering two distinct flight formation modes: follow formation and helix formation. Leveraging interferometric altimetry and differential deformation measurement technologies, they can fulfill global high-precision, all-time, and all-weather tasks such as topographic mapping, surface deformation monitoring, and geological hazard monitoring. GF-7 satellite was successfully launched in China on November 3, 2019. Equipped with a dual-beam laser altimeter, it emits laser pulses with a wavelength of 1064 nm to the ground at a working frequency of 3 Hz, forming discrete laser footprints on the ground with an along-track spacing of approximately 2.4 km and a cross-track spacing of about 12.25 km.

In this study, high-precision laser altimetry points (LAPs) extracted from GF-7 SLA03 data are adopted as verification benchmark, and statistical analysis and error analysis are employed to conduct a cross-validation of the elevation accuracy of LT-1 raw DEM (LT-1 RDEM), SRTM, TanDEM-X DEM (TanDEM) and ZY-3 DEM. Based on geomorphological classification, four typical landform types—plain, platform, hill, and mountain—are selected as study areas for quantitative accuracy assessment. Using the height error and the root mean square error (RMSE) as key metrics, the elevation accuracy performance of each DEM across these four landform types is analyzed.

This contribution has been peer-reviewed. The double-blind peer-review was conducted on the basis of the full paper.
https://doi.org/10.5194/isprs-annals-XI-1-2026-131-2026

2. Methodology

2.1 Application of InSAR Technology in LT-1 RAW DEM

The principle of InSAR-derived DEMs is to obtain the phase difference at the same surface location caused by differences in satellite positions by performing interferometric processing on the phase information of SAR images acquired at the same location but different times (Y. Lu et al., 2020). The helix formation of LT-1 can image the same ground location simultaneously, eliminating temporal decorrelation effects, and the elevation values can be calculated using the phase difference between the same surface location and the dual-satellite antennas. During the production of LT-1 RDEM, the technical workflow mainly includes the following steps: interferometric pair co-registration and resampling, differential interferometry for fringe pattern generation, removal of flat-earth and topographic phase, interferogram filtering, phase unwrapping, fine baseline estimation, phase-to-height conversion and geocoding.

2.2 Height System Transformation

The four DEMs share the same horizontal reference datum (WGS-84), but their vertical datums are inconsistent. Among them, SRTM adopts the orthometric height system with the EGM96 geoid model, while LT-1 RDEM, TanDEM, and ZY-3 DEM use the ellipsoidal height system. Therefore, it is necessary to unify the vertical datum before conducting comparative analysis. The conversion between ellipsoidal height and orthometric height is given by:

$$h = H + N, \tag{1}$$

where h represents the ellipsoidal height at a given location, H denotes the corresponding orthometric height, and N is the geoid undulation, which can be derived from the relevant geoid model. In this study, all DEMs and reference data are unified to the WGS84 ellipsoidal height datum

2.3 Accuracy Assessment

This study evaluates the elevation accuracy of the four DEMs based on height error (HE) and RMSE. The height error is calculated as:

$$HE = H_i - H_i', \tag{2}$$

where H_i is the elevation value from the DEM at the location of the *i-th* LAP, and H_i' is the elevation value of the *i-th* LAP itself.

The RMSE is computed as:

$$RMSE = \sqrt{\frac{\sum_{i=1}^{N} \left(H_i - H_i'\right)^2}{N}}, \tag{3}$$

where N is the total number of GF-7 LAPs in the study area.

3. Experimental Results and Discussion

3.1 Experimental data

DEMs derived from InSAR data are essentially digital surface models (DSM); therefore, the three InSAR-derived DEMs in this study also refer to DSMs. The LT-1 RDEM used in this research is extracted from the helix formation data of the LT-1 mission acquired between September 30th and November 25th, 2022, with a ground resolution of 10 meters. It is designated as raw DEM because it was not processed with ground control points or refined through manual editing and other post-processing steps. SRTM adopts Version 4.1 with a 90-meter ground resolution, released in 2018, which is based on the finished-grade 2006 SRTM v2 release by NASA and was post-processed and published in 2008 by CGIAR-CSI. The TanDEM utilized in this study is the 90-meter resolution version released in 2016, a product variant of the global DEM acquired under Germany’s TanDEM-X mission framework from 2010 to 2015. This version is unedited without void filling or interpolation. The ZY-3 DEM employed is the 10-meter resolution 2020 version, produced based on data from China’s civil high-resolution optical transmission-type stereo mapping satellite. The GF-7 SLA03 data is a standardized laser altimetry product formed after systematic processing. In the data, LAPs marked with ECP_Flag values of 1, 2, or 3 have a theoretical accuracy better than 1 meter and can be used as verification benchmark in this study to validate the accuracy of the DEMs

To evaluate the elevation accuracy and performance across different landform types of four DEMs—LT-1 RDEM, SRTM, TanDEM, and ZY-3 DEM—Guyuan County in Hebei Province, China, was selected as the study area. Covering approximately 3,654 km², the county encompasses four distinct geomorphological types—plain, platform, hill, and mountain—as identified in the 1:1 million Digital Geomorphological Dataset of China. A total of 745 LAPs were selected from the GF-7 SLA03 data within the study area, filtered based on ECP_Flag values of 1, 2, or 3. The spatial distribution of these LAPs is shown in Figure 1.

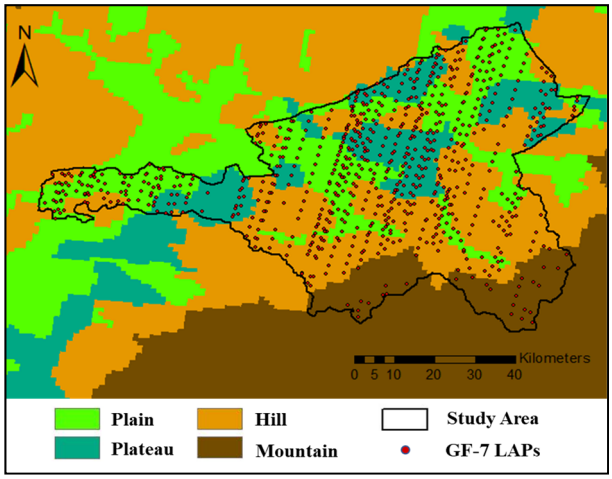

Figure 1. Study area.

3.2 Results and Discussion

This study first conducted a visual comparison of the four DEMs, generated hillshade models of the four DEMs in the study area, and rendered them after overlaying with the DEMs. The results are shown in Figure 2.

It can be seen from Figure 2(a) that: benefiting from the 10-meter resolution, LT-1 RDEM and ZY-3 DEM exhibit more detailed texture features compared with TanDEM and SRTM (both with 90-meter resolution). In Figure 2(b), TanDEM and SRTM perform poorly in presenting topographic texture details. Both LT-1 RDEM and ZY-3 DEM can reveal more distinct topographic undulations in the hilly areas on the east and west sides, while in the central plain area, LT-1 RDEM offers richer

surface details. However, since LT-1 RDEM has not undergone subsequent refined processing such as manual editing, it inevitably contains noise.

This study calculated the mean HE and RMSE between the four DEMs and GF-7 LAPs across four different landform types, respectively. The results are shown in Table 1. In addition, the height error distributions of the four DEMs relative to GF-7 LAPs under different landform types were statistically analyzed, and histograms were plotted (Figure 3). Furthermore, to explore the penetration capability of different payloads of the experimental data, referring to the forest cover information from GLC_FCS30-2020 (a 2020 global 30m fine-resolution land cover classification product released by the research team led by Researcher Liu Liangyun from the Aerospace Information Research Institute, Chinese Academy of Sciences), the experimental area was simplified into three landcover classifications: forest, non-forest, and water body. The values of the four DEMs were extracted along the red straight line in Figure 4 (the line was resampled into points with a 10-meter interval), and scatter plots were generated (Figure 5).

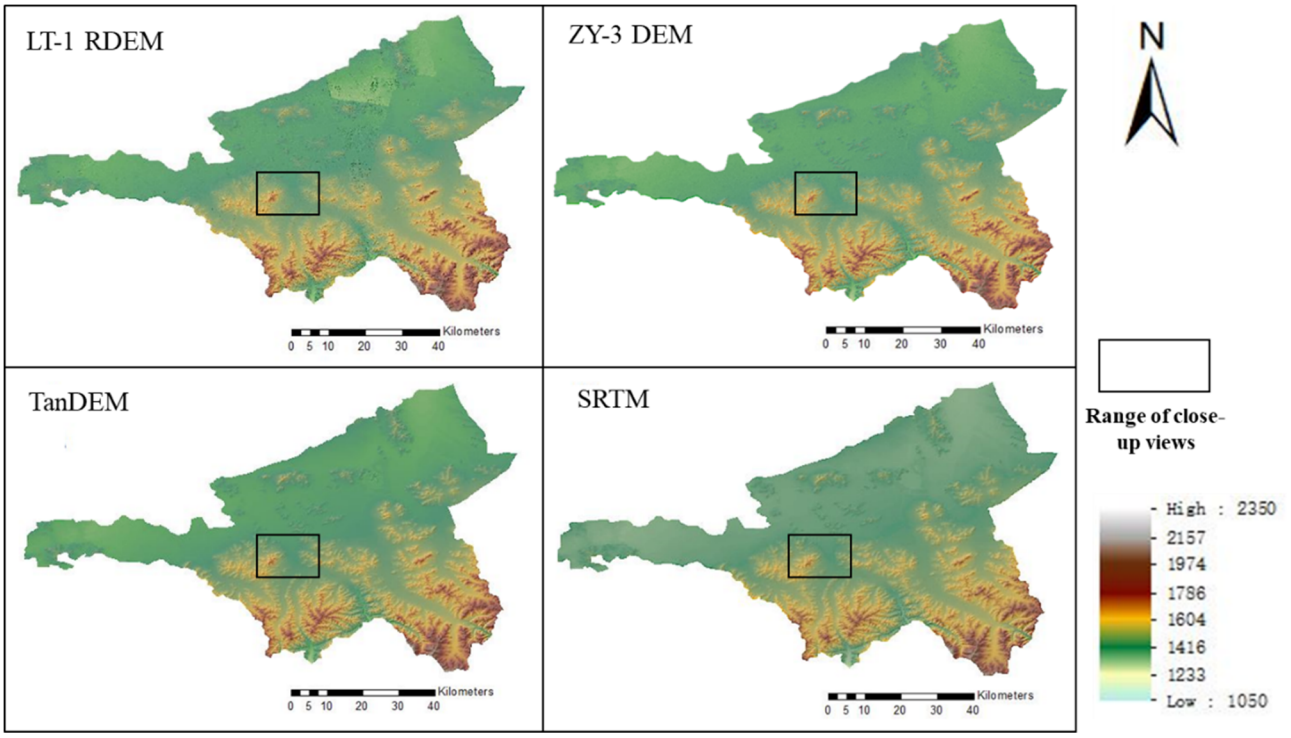

(a) Overviews

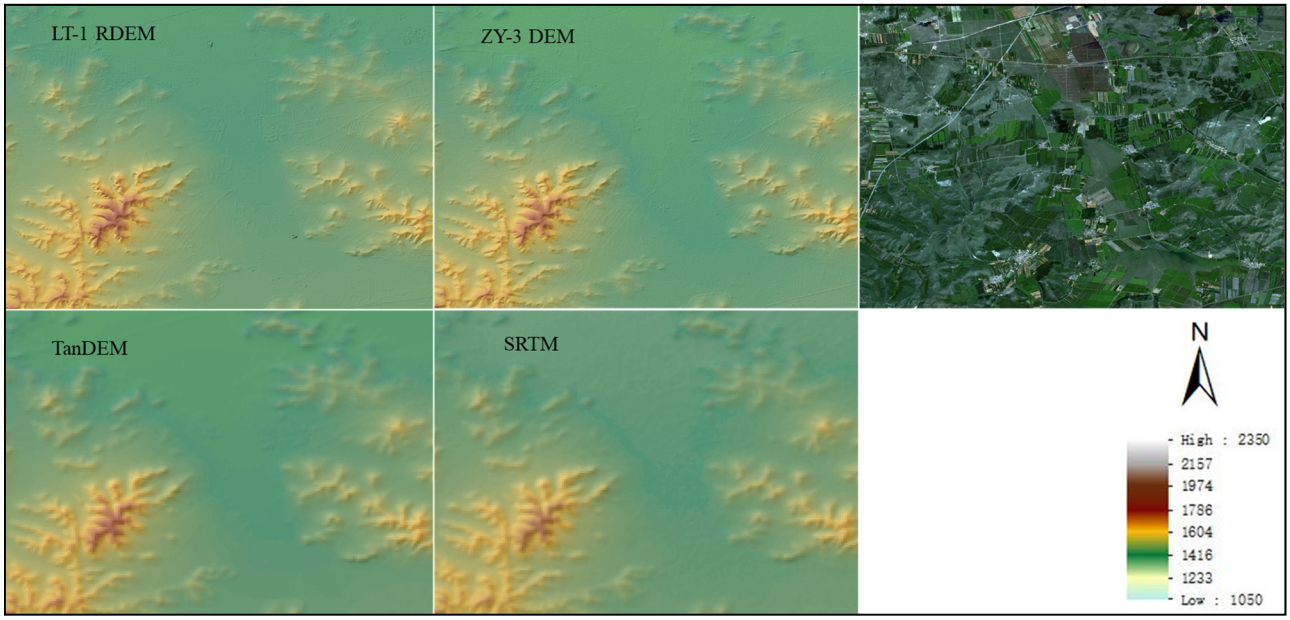

(b) Close-up views and optical images

Figure 2. Rendered maps of the four DEMs in the study area.

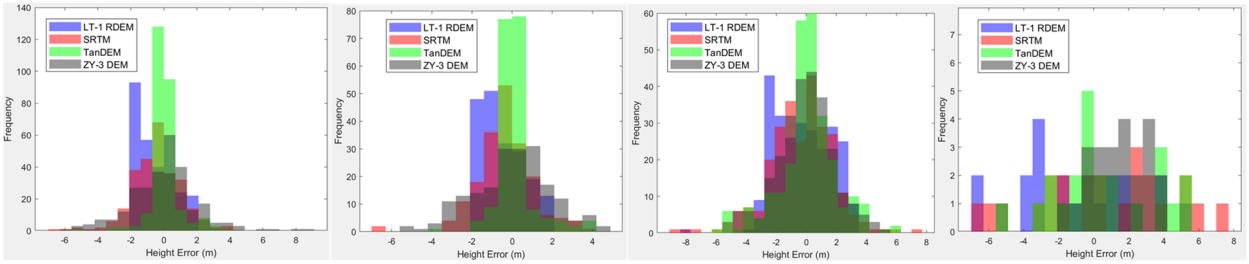

(a) Plain (b) Hill (c) Plateau (d) Mountain

Figure 3. Distribution of height errors (DEMs - GF-7 LAPs).

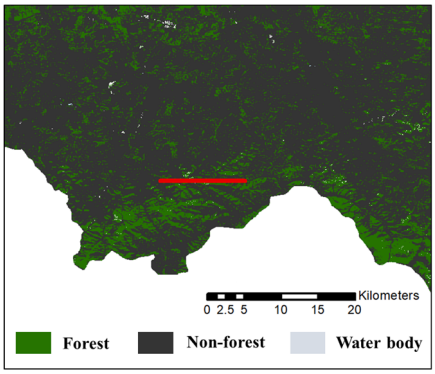

Figure 4. Location of the DEMs' scatter plot

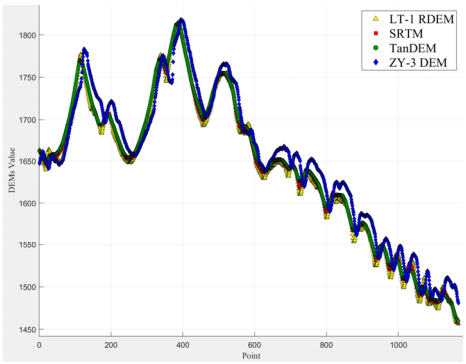

Figure 5. Scatter plot of DEM values

Type		Plain	Hill	Plateau	Mountain	Study Area
	GF-7 LAPs	272	192	258	23	745
LT-1 RDEM	**Mean Error (m)**	-0.606	-0.486	-0.345	-1.001	-0.610
	RMSE (m)	1.130	1.180	1.924	3.427	1.958
SRTM	**Mean Error (m)**	-0.441	-0.361	-0.357	0.585	-0.143
	RMSE (m)	1.574	1.469	2.194	3.784	2.255
TanDEM	**Mean Error (m)**	0.048	0.136	0.082	0.588	0.214
	RMSE (m)	0.907	0.944	1.925	2.825	1.650
ZY-3 DEM	**Mean Error (m)**	0.003	0.014	0.026	1.345	0.349
	RMSE (m)	2.149	1.916	1.798	2.033	1.974

Table 1. Elevation accuracy of the experimental DEMs across different landform types

It can be concluded from the analysis of Table 1, Figure 3, and Figure 5 that LT-1 RDEM performs best in depicting topographic texture details and has the strongest payload penetration capability. When taking GF-7 LAPs as the verification benchmark, the elevation accuracy of LT-1 RDEM is second only to TanDEM. Specifically:

(1) Across the entire study area, the RMSE of height errors between the four DEMs and GF-7 LAPs are 1.958m, 2.255m, 1.65m, and 1.974m in sequence. It can be seen that the RMSE of LT-1 RDEM is smaller than that of SRTM and ZY-3 DEM, but slightly larger than that of TanDEM—indicating that TanDEM’s elevation values are closer to GF-7 LAPs. However, LAPs extracted from GF-7 laser data may be obstructed by buildings or vegetation, resulting in non-ground points and thus overestimated elevations. Meanwhile, the RMSE of the four DEMs generally increases in the order of plains, tablelands, hills, and mountains, reflecting that the elevation accuracy of DEMs varies under different topographic conditions.

(2) Whether considering the average errors in plains, tablelands, hills, and mountains, or the overall average error across all landform types, the values of ZY-3 DEM and TanDEM are both positive and relatively close. The error histograms for the four landform types show that the two have more similar distribution patterns, with height differences mainly concentrated in the region greater than 0. Therefore, ZY-3 DEM and TanDEM have good consistency, and their payloads basically lack the ability to penetrate surface objects.

(3) The overall average error of SRTM is -0.143m, slightly lower than TanDEM’s 0.214m and ZY-3 DEM’s 0.349m. The values in the error histogram are mainly concentrated in the region less than 0, indicating that SRTM’s payload has a certain degree of penetration capability.

(4) LT-1 RDEM has the smallest overall average error (-0.61m), and its height difference distribution histogram also shows that the number of height differences less than 0 is much larger than that of the other three DEMs. Meanwhile, the area where the scatter plot (Figure 5) is located features an alternating distribution of non-forest-covered areas and forest-covered areas, and the elevation values of LT-1 RDEM (represented by yellow triangles) are significantly lower than those of the other

This contribution has been peer-reviewed. The double-blind peer-review was conducted on the basis of the full paper.
https://doi.org/10.5194/isprs-annals-XI-1-2026-131-2026 | © Author(s) 2026. CC BY 4.0 License.

three DEMs, demonstrating that LT-1 has the strongest payload penetration capability.

4. Conclusions

This study systematically evaluated the accuracy performance of four DEMs (LT-1 RDEM, SRTM, TanDEM, and ZY-3 DEM) in the typical landform area of Guyuan County, Hebei Province, China, using LAPs obtained from GF-7 satellite laser altimetry data as the verification benchmark. Through quantitative error analysis and statistics, the following conclusions are drawn:

(1) There are significant differences in the accuracy of DEM products, which are closely related to landform types. Overall, the accuracy generally increases in the order of plains, tablelands, hills, and mountains. This indicates that topographic complexity is a key factor affecting DEM accuracy, and geometric distortion caused by topographic undulations is the main reason for the decreased accuracy in mountainous and hilly areas.

(2) Visual comparison shows that the 10-meter resolution LT-1 RDEM has obvious advantages in depicting topographic texture details and can more clearly show subtle geomorphic features. However, as uncontrolled and unrefined raw DEM data, its absolute accuracy needs to be improved.

(3) Error statistics indicate that the L-band LT-1 RDEM has negative average errors under all four landform types, with elevation differences densely distributed near zero. This phenomenon strongly proves that the L-band radar signal of LT-1 has stronger penetration capability compared with the C-band (SRTM) and X-band (TanDEM), and the elevation values obtained are likely closer to the true ground point elevations, especially showing significant characteristics in mountainous areas.

(4) Although this study confirms that TanDEM exhibits the optimal accuracy when using GF-7 LAPs as verification benchmark, it must be recognized that when GF-7 laser altimetry data encounters buildings or dense vegetation canopies, the returned elevation may not be the true ground elevation. This characteristic may lead to systematic overestimation of the elevation accuracy of DEM products. Therefore, in the absence of ground measured data, a cautious attitude should be adopted towards the "optimal" accuracy conclusions derived from such verification sources.

This study shows that the domestic LT-1 RDEM has great potential in terms of resolution and penetration capability. An important research direction in the future is to develop and optimize post-processing algorithms for LT-1 data to fully tap its data potential, produce DEM products with both high detail expression and high accuracy, and serve economic development and scientific research.

Acknowledgements

This study was supported by NSFC (41671440), and 2016 National Key Research and Development Plan of China (2016YFC0803103).

References

Apeh, O., Uzodinma, V., Ebinne, E., Moka, E., & Udochukwu Onah, E., 2019: Accuracy Assessment of Alos W3d30, Aster Gdem and Srtm30 Dem: A Case Study of Nigeria, West Africa. *Journal of Geographic Information System, 11*, 111-123. doi:10.4236/jgis.2019.112009

Eldhuset, K., Andersen, P. H., Hauge, S., Isaksson, E., & Weydahl, D. J., 2003: ERS tandem InSAR processing for DEM generation, glacier motion estimation and coherence analysis on Svalbard. *International Journal of Remote Sensing, 24*(7), 1415-1437. doi:10.1080/01431160210153039

Hong, D.-B., & Yang, C.-S., 2018: Automatic discrimination approach of sea ice in the Arctic Ocean using Sentinel-1 Extra Wide Swath dual-polarized SAR data. *International Journal of Remote Sensing, 39*(13), 4469-4483. doi:10.1080/01431161.2017.1415486

Karabörk, H., Makineci, H. B., Orhan, O., & Karakus, P., 2021: Accuracy Assessment of DEMs Derived from Multiple SAR Data Using the InSAR Technique. *Arabian Journal for Science and Engineering, 46*(6), 5755-5765. doi:10.1007/s13369-020-05128-8

Leonardo, E. M. C., Watt, M. S., Pearse, G. D., Dash, J. P., & Persson, H. J., 2020: Comparison of TanDEM-X InSAR data and high-density ALS for the prediction of forest inventory attributes in plantation forests with steep terrain. *Remote Sensing of Environment, 246*, 111833. doi:https://doi.org/10.1016/j.rse.2020.111833

Li, H., Zhao, J., Yan, B., Yue, L., & Wang, L., 2022: Global DEMs vary from one to another: an evaluation of newly released Copernicus, NASA and AW3D30 DEM on selected terrains of China using ICESat-2 altimetry data. *International Journal of Digital Earth, 15*(1), 1149-1168. doi:10.1080/17538947.2022.2094002

Li, T., Tang, X., Gao, X., Zhang, X., Zhang, X., Lu, J., . . . Li, Z., 2023: Lu Tan-1 SAR satellite characteristics and productions in the phase of in-orbit test. *Int. Arch. Photogramm. Remote Sens. Spatial Inf. Sci., XLVIII-1/W2-2023*, 1251-1256. doi:10.5194/isprs-archives-XLVIII-1-W2-2023-1251-2023

Liu, X., Peterson, J., & Zhang, Z., 2005: *High-resolution DEM generated from LiDAR data for water resource management*.

Lu, H., Suo, Z., Li, Z., Xie, J., Zhao, J., & Zhang, Q., 2018: InSAR Baseline Estimation for Gaofen-3 Real-Time DEM Generation. *Sensors, 18*(7), 2152. Retrieved from https://www.mdpi.com/1424-8220/18/7/2152

Lu, Y., Zhang, J., Tong, X., Lu, X., Han, W., Zhang, H., . . . Liu, X., 2020: Selection of persistent scatterer interferometric synthetic aperture radar master image considering temporal baseline, spatial baseline and doppler centroid frequency difference. *ISPRS Annals of Photogrammetry, Remote Sensing and Spatial Information Sciences, V-3-2020*, 141-148. doi:10.5194/isprs-annals-V-3-2020-141-2020

Shangmin, Z., Weiming, C., Jingtian, J., & Wenjuan, S. H. A., 2020: Error Comparison among the DEM Datasets Made from ZY-3 Satellite and the Global Open Datasets. *Journal of Geo-information Science, 22*(3), 370-378. doi:10.12082/dqxxkx.2020.190658

Shuangcheng, Z., Jie, W., Tao, L. I., Wu, Z. H. U., Yufen, N. I. U., Chuhan, Z., . . . Zhenhong, L. I., 2025: The accuracy verification and analysis of the interferometry of the LT-1 satellite——a case study of Datong. *Geomatics and Information*

Science of Wuhan University, 0(0). doi:10.13203/j.whugis20240424

Takaku, J., Tadono, T., Tsutsui, K., & Ichikawa, M., 2016: Validation of "AW3D" global DSM generated from ALOS prism. *ISPRS Ann. Photogramm. Remote Sens. Spatial Inf. Sci., III-4*, 25-31. doi:10.5194/isprs-annals-III-4-25-2016

Tang, X., Li, S., Li, T., Gao, Y., Zhang, S., Chen, Q., & Zhang, X., 2021: Review on global digital elevation products. *National Remote Sensing Bulletin, 25*, 167-181. doi:10.11834/jrs.20210210

Uuemaa, E., Ahi, S., Montibeller, B., Muru, M., & Kmoch, A., 2020: Vertical Accuracy of Freely Available Global Digital Elevation Models (ASTER, AW3D30, MERIT, TanDEM-X, SRTM, and NASADEM). *Remote Sensing, 12*(21), 3482. Retrieved from https://www.mdpi.com/2072-4292/12/21/3482

Wecklich, C., Martone, M., Rizzoli, P., Bueso-Bello, J. L., Gonzalez, C., & Krieger, G., 2017: *Production of a global forest/non-forest map utilizing TanDEM-X interferometric SAR data.* Paper presented at the 2017 IEEE International Geoscience and Remote Sensing Symposium (IGARSS).

Wei, Z., Er-xue, C., Guolin, L., Wenmei, L., & Qi, F., 2013: *Extract DEM from ALOS based on Polarimetric SAR interferometry*.

Zhao, S., Cheng, W., Zhou, C., Chen, X., Zhang, S., Zhou, Z., . . . Chai, H., 2011: Accuracy assessment of the ASTER GDEM and SRTM3 DEM: an example in the Loess Plateau and North China Plain of China. *International Journal of Remote Sensing, 32*(23), 8081-8093. doi:10.1080/01431161.2010.532176